Oil & Natural Gas Technology

DOE Award No.: DE-FE0013889

Quarterly Research Performance Progress Report (Period ending 03/31/2015)

THCM Coupled Model For Hydrate-Bearing Sediments: Data Analysis and Design of New Field Experiments (Marine and Permafrost Settings)

Project Period (10/1/2013 to 09/30/2015)

Submitted by:

Marcelo Sanchez Project PI

Texas A&M University
DUNS #: 847205572
College Station, TX
979-862-6604
msanchez@civil.tamu

J. Carlos Santamarina

Georgia Institute of Technology
Atlanta, Georgia
404-894-7605
edujcs@gatech.edu

Prepared for:
United States Department of Energy
National Energy Technology Laboratory
Submission date: 05/08/2015

NETL

Office of Fossil Energy

DISCLAIMER

ACCOMPLISHMENTS

The experimental study of hydrate bearing sediments has been hindered by the very low solubility of methane in water (lab testing), and inherent sampling difficulties associated with depressurization and thermal changes during core extraction. This situation has prompted more decisive developments in numerical modeling in order to advance the current understanding of hydrate bearing sediments, and to investigate/optimize production strategies and implications. The goals of this research is to addresses the complex thermo-hydro-chemo-mechanical THCM coupled phenomena in hydrate-bearing sediments, using a truly coupled numerical model that incorporates sound and proven constitutive relations, satisfies fundamental conservation principles. This tool will allow us to better analyze available data and to further enhance our understanding of hydrate bearing sediments in view of future field experiments and the development of production technology.

ACCOMPLISHED

The project management plan (PMP, Task 1) and the selection of the PhD Students working during the 1st year of the project were competed and informed in the first quarterly report. The main accomplishments for this first period address Tasks 2, 3 and 4 of the original research plan, and include:

- Student training.
- Literature review.
- Update of constitutive equations.
- Update of THCM-Hydrate.
- Close-form analytical solutions.
- Numerical analyses

Training

The training of the two PhD students working in this project has continued during this period. As for Mr. Xuerui (Gary) Gai (i.e. the Ph.D. student at TAMU), he is progressing in the modeling of problems involving has hydrate sediments. As for Mr. Zhonghao Sun (the Ph.D. student at GT), he has continued with the implementation of analytical solutions in MATLAB and other pieces of software. Both students have progressed positively with their coursework at their respective universities.

Literature review

The literature review (Task 2) was completed in a previous period.

Update of Update of THCM-Hydrate

The update of the constitutive laws for hydrate-bearing marine sediments and HBS in the permafrost (i.e. Task 3) was completed in a previous period.

Close-form analytical solutions

The review on the main governing evolution laws, parameters, dimensionless ratios and simplifying assumptions for HBS dissociation (i.e. Task 4) was completed in this period.

Numerical analyses

The numerical analyses solving field production experiments as boundary value problems have been continued in this period.

A mechanical model has been studied and a numerical algorithm for its implementation has been developed. The main results are presented in page 6.

The numerical solution of the benchmark #2 and the comparisons between THCM-Hydrate and other numerical codes is presented in page10.

Plan - Next reporting period

We will advance analytical and numerical fronts to enhance our code to solve coupled THCM problems involving with HBS, with renewed emphasis on simulating the natural processes under *in-situ* conditions and gas production.

Milestones for each budget period of the project are tabulated next. These milestones are selected to show progression towards project goals.

	Milestone Title Planned Date and Verification Method	Actual Completion Date	Comments
Title Related Task / Subtasks Planned Date Verification method	Complete literature review 2.0 / 2.a March 2014 Report	March 2014	Completed
Title Related Task / Subtasks Planned Date Verification method	Complete updated Constitutive Equations 2.0 / 2.b & 2.c June 2014 Report (with preliminary validation data)	July 2014	Completed
Title Related Task / Subtasks Planned Date Verification method	Validate new THCM constitutive equations 3.0 / 3.a, 3.b & 3.c September 2014 Report (with first comparisons between experimental and numerical results)	September 2014	Completed
Title Related Task / Subtasks Planned Date Verification method	Complete close-form analytical solutions 4.0 / 4.a & 4.b February 2015 Report (with analytical data)	February 2015	Completed
Title Related Task / Subtasks Planned Date Verification method	Complete numerical analyses 5.0 / 5.a, 5.b & 5.c July 2015 Report (with analytical and numerical data)	July 2015	Progressing as planned
Title Related Task / Subtasks Planned Date Verification method	Complete THCM-Hydrate code modifications 6.0 / 6.a June 2015 Report (with numerical data)	June 2015	Progressing as planned
Title Related Task / Subtasks Planned Date Verification method	Complete production optimization 7.0 / 7.a, 7.b, 7.c, 7.d & 7.e September 2015 Report (with numerical data)	September 2015	Progressing as planned

Modeling the Mechanical Behavior of Gas Hydrate Bearing Sediments

The mechanical response of hydrate bearing sediments (HBS) is highly complex and dependent on thermo, hydraulic and geo-chemical coupled interactions. Furthermore, HBS behavior is also affected (amongst others) by, sediment type, stress level, gas hydrate morphology and sediment history. Significant volume changes are anticipated during hydrate dissociation/formation. Those changes are basically controlled by the mechanical stability of the soil structure hosting the hydrate. The mechanical model is a crucial component for a proper description of this problem, as it relates volume (and porosity) changes with: fluids pressure, temperature, chemical and stress variations. A good prediction of stresses is critical for a reliable assessment of (amongst others) borehole stability and sediment integrity.

Most of the numerical simulations involving HBS have been performed using rather simpler mechanical constitutive equations (i.e. generally based on elastic or perfect plastic Mohr Coulomb models) that are not able to capture the complex behavior of HBS. The quite limited experimental data associated with the mechanical behavior of HBS was perhaps one of the main reason that hindered the development of more realistic geomechanical models. However, there have been a number of recent experimental investigations related to the geomechanical behavior of course-grained (sandy) sediments (e.g. Hyodo at al., 2005; 2008; Masui et al., 2008; Yoneda et al., 2010) that have been used to develop more realistic mechanical constitutive models for HBS (e.g. Miyazaki et al., 2012; Pinkert.et al., 2014; Uchida et al., 2012). The critical state model proposed by the Uchida et al. (2012) is perhaps the more advanced constitutive equation for HBS. This model is based on the Modified Cam-Clay (MCC) framework. This constitutive equation adds the main following components to the MCC model: sub-loading concepts; cementing effects associated with the presence of hydrates; impact of hydrate saturation on shear strength; and bonding damage.

The model proposed by Uchida et al. (2012) has been adopted in this research to enhance it by including additional phenomena associated with HBS behavior. The main components of Uchida et al. (2012) model is presented in Section 1, the validation of the numerical algorithm implemented in this project is presented in Section 2. Further developments will be presented in subsequent reports.

1 Model definition

The starting point of the mechanical constitutive model for HBS presented in this section is the MCC model (i.e. Roscoe et al., 1958; Roscoe and Burland, 1968). The main ingredients of the Uchida et al. (2012) constitutive equation is presented below, starting by the MCC model.

Modified Cam-Clay Model

The increment of the elastic volumetric strains depend on the increment of the mean effective stress (*p'*) through the stress-dependent elastic soil bulk modulus *K':*

$$K' = \frac{\nu}{\kappa} p' \tag{1}$$

where ν is the specific volume (ν =1+*e*, where *e* is the void ratio); and κ is the slope of the unloading/reloading line. Deviatoric elastic strains and stresses relate through the shear modulus (*G*). The yield function (*f*) defines the limit of the elastic domain. In the MCC model an ellipse is adopted to define *f*, as follows:

$$f = \frac{q^2}{M^2} + p'^2 - p' p_c \tag{2}$$

where *q* is the deviatoric stress, *M* is the slope of critical line in the *q-p'* space; p_c' is the effective pre-consolidation pressure; which is the hardening variable of this model. It is assumed that the hardening law is isotopic and dependent on the plastic volumetric strain (ε_v^p) through:

$$\frac{dp_c}{p_c} = \frac{\nu}{\lambda - \kappa} d\varepsilon_v^p \tag{3}$$

where λ is the slope of the normal compression line.

An associated flow rule is assumed in this model (i.e. *f* coincide with the plastic potential *g*), so the flow rule can be simply written as:

$$d\boldsymbol{\varepsilon}^p = \Lambda \frac{\partial \mathrm{g}}{\partial \boldsymbol{\sigma}} = \Lambda \frac{\partial \mathrm{f}}{\partial \boldsymbol{\sigma}} \tag{4}$$

where Λ is the plastic multiplier and $\boldsymbol{\sigma}$ is the effective Cauchy's stress tensor.

Hydrate Strength Enhancement and Bonding Damage

An additional mechanism is added to the MCC model to account for the increase of strength observed in hydrate bearing sediments. This phenomenon can be associated with a sort of cementing effect induce by the presence of gas hydrates in the pore structure. This mechanism will induce an isotropic expansion of the yield surface, with the related enhancement of sediment strength. This effect is defined through the following evolution law:

$$\mathrm{p_d} = \mathrm{a}\left(\chi\ \mathrm{S_H}\right)^{\mathrm{b}} \tag{5}$$

where p_d is an additional hardening parameter that controls the increase of the sediment strength associated with the presence of hydrates; S_H is hydrate saturation; *a* and *b* are constants that describe the degree of hydrate contribution to the hardening parameter; and χ is a damage factor that varies between 1 (maximum bonding effect provided by the hydrate) and 0 (no bonding effect). It is assumed that the strength enhancement can be degraded during yielding. This effect is incorporated by defining the following evolution law for χ:

$$d\chi = -r\,\chi\,d\varepsilon_q^p \tag{6}$$

where r is a parameter that defines the rate of mechanical damage and $d\varepsilon_q^p$ is the plastic deviatoric strain.

Enhanced Yield Function for Modeling HBS

The yield function of the MCC model incorporating the strength enhancement effect provided by the presence of gas hydrate can be written as:

$$f = \frac{q^2}{M^2} + p'^2 - p'\left(p_c + p_d\right) \tag{7}$$

The MCC model assumes that plastics strains only occur when the stresses reach the yield surface. However, in some sediments irrecoverable strains are also observed when the stress state is inside the yield surface. It is also well-known that the MCC model predicts a sharp transition between elastic and plastic states (particularly in soils with dilatancy). Sub-loading concepts can be incorporated in the formulation of the constitutive equations to overcome these two limitations of the MCC model (Uchida et al., 2012). According to Hashiguchi (1989) the sub-loading surface ratio *R* (with $0 < R \le 1$) can be incorporated in the definition of the yield surface, leading to:

$$f = \frac{q^2}{M^2} + p'^2 - R\,p'\left(p_c + p_d\right) \tag{8}$$

where the changes in *R* are defined through the following evolution law:

$$\mathrm{dR} = -\mathrm{u}\,\ln\mathrm{R}\left|d\varepsilon^p\right| \tag{9}$$

where $|d\varepsilon^p|$ is the norm of the (total) plastic strain vector and *u* is a sub-loading parameter that controls the plastic deformations before yielding. Through this plastic mechanism it is possible to model the irreversible strains generally observed when the stress sate is inside the yield surface and also to introduce smooth transition between elastic and plastic conditions.

HBS Model - Stress-Strain Relationship

To ensure that the stress state remains on the yield surface during yielding the consistency condition is enforced:

$$df = \frac{\partial \mathrm{f}}{\partial \boldsymbol{\sigma}} : d\boldsymbol{\sigma} + \frac{\partial \mathrm{f}}{\partial \mathrm{p}_c} d\mathrm{p}_c + \frac{\partial \mathrm{f}}{\partial \mathrm{R}} d\mathrm{R} \tag{10}$$

By substituting the flow rule (4) into the consistency condition (10), the plastic multiplier can be expressed as:

$$\Lambda = \frac{\dfrac{\partial \mathrm{f}}{\partial \boldsymbol{\sigma}} : d\boldsymbol{\sigma} + \dfrac{\partial \mathrm{f}}{\partial \mathrm{p}_d} a\, b\left(\chi\, S_H\right)^{b-1} \chi\, dS_H}{\dfrac{\partial \mathrm{f}}{\partial \mathrm{p}_c} \dfrac{v}{\lambda - \mathrm{k}} p_c \dfrac{\partial \mathrm{f}}{\partial \mathrm{p}} + \dfrac{\partial \mathrm{f}}{\partial \mathrm{p}_d} a\, b(-r)\left(\chi\, S_H\right)^{b} \dfrac{\partial \mathrm{f}}{\partial \mathrm{q}} + \dfrac{\partial \mathrm{f}}{\partial \mathrm{R}}(-\mathrm{u})\ln\mathrm{R}\left|\dfrac{\partial \mathrm{f}}{\partial \boldsymbol{\sigma}}\right|} \tag{11}$$

The effective stress-strain relationship can be obtained after multiplying the elastic constitutive matrix ($\mathbf{D}^e$) time the elastic strains; which in turns can be obtained as the difference between the total and the plastic strains, as follows:

$$d\boldsymbol{\sigma} = \mathbf{D}^e \left(d\boldsymbol{\varepsilon} - \Lambda \frac{\partial \mathrm{f}}{\partial \boldsymbol{\sigma}} \right) \tag{12}$$

After some algebra, the constitutive relationship can be expressed as:

$$d\boldsymbol{\sigma} = \mathbf{D}_{\varepsilon} d\boldsymbol{\varepsilon} + \mathbf{D}_{s_H} dS_H \tag{13}$$

where:

$$\mathbf{D}_{\varepsilon} = \left[\mathbf{D}^e - \frac{\mathbf{D}^e \dfrac{\partial \mathrm{f}}{\partial \boldsymbol{\sigma}} \left(\dfrac{\partial \mathrm{f}}{\partial \boldsymbol{\sigma}}\right)^T \mathbf{D}^e}{\left(\dfrac{\partial \mathrm{f}}{\partial \boldsymbol{\sigma}}\right) \mathbf{D}^e \dfrac{\partial \mathrm{f}}{\partial \boldsymbol{\sigma}} + \dfrac{\partial \mathrm{f}}{\partial \mathrm{p}_c} \dfrac{v}{\lambda - \mathrm{k}} p_c \dfrac{\partial \mathrm{f}}{\partial \mathrm{p}} + \dfrac{\partial \mathrm{f}}{\partial \mathrm{p}_d} a\, b(-r)\left(\chi\, S_H\right)^{b} \dfrac{\partial \mathrm{f}}{\partial \mathrm{q}} + \dfrac{\partial \mathrm{f}}{\partial \mathrm{R}}(-\mathrm{u})\ln\mathrm{R}\left|\dfrac{\partial \mathrm{f}}{\partial \boldsymbol{\sigma}}\right|} \right] \tag{14}$$

$$\mathbf{D}_{SH} = \left[\mathbf{D}^e \frac{\dfrac{\partial \mathrm{f}}{\partial \mathrm{p}_d} a\, b\left(\chi S_H\right)^{b-1} \chi}{\dfrac{\partial \mathrm{f}}{\partial \mathrm{p}_c} \dfrac{v}{\lambda - \mathrm{k}} p_c \dfrac{\partial \mathrm{f}}{\partial \mathrm{p}} + \dfrac{\partial \mathrm{f}}{\partial \mathrm{p}_d} a\, b(-r)\left(\chi S_H\right)^{b} \dfrac{\partial \mathrm{f}}{\partial \mathrm{q}} + \dfrac{\partial \mathrm{f}}{\partial \mathrm{R}}(-\mathrm{u})\ln\mathrm{R}\left|\dfrac{\partial \mathrm{f}}{\partial \boldsymbol{\sigma}}\right|} \right] \tag{15}$$

2 Model Application

The model presented in the previous section has been implemented using a strain-control algorithm. Following a similar approach to Uchida et al. (2012), the model implementation was first validated using experimental tests already published by Masui et al. (2005). Masui et al. (2005) conducted several triaxial compression tests using synthetic methane hydrate specimens. Three hydrate accumulation habits have been distinguished in the literature (e.g. Waite et al., 2012) namely: pore filling, load bearing, and cementing. The specimens containing synthetic methane hydrate were produced from two types of host specimen mixture of Toyoura sand with ice (ice-seed method) and/or with water (partial water saturation method). It can be anticipated that the ice-seed method will produce gas hydrates where the pore-filling habit is dominant, and that the partial water saturation method will form hydrates sediments where the cementing habit will be predominant. The sediments formed using the two methods were confined in a triaxial pressure vessel that replicates the pore pressure conditions equivalent to a depth of approximately 800m under the sea. Drained tests were run under a constant temperature of 278 °K and an effective confining pressure of 1.0 MPa.

In order to validate the sub-loading model, first a triaxial compression test using pure Toyoura sand (i.e. with no synthetic hydrate formed in the sample) was selected from Masui et al. (2005). Simulations were conducted using the MCC and sub-loading models to compare their perfomance. Figure 1.a shows the stress-strain behavior and Figure 1.b presents the volumetric response of Toyoura sands, experimental results are presented with symbols (Masui et al. 2005). Modeling results obtained with the MCC and sub-loading models are also presented. It is clear that the sub-loading model is able to capture very satisfactorily the main features of HBS response, with smooth transition between elastic and plastic behaviors. The MCC model manages to replicate well the residual strength, but over-predicts the maximum strength and also the dilatancy of the soil. It also presents a sharp transition between elastic and elasto-plastic states, aspect that is not very realistic.

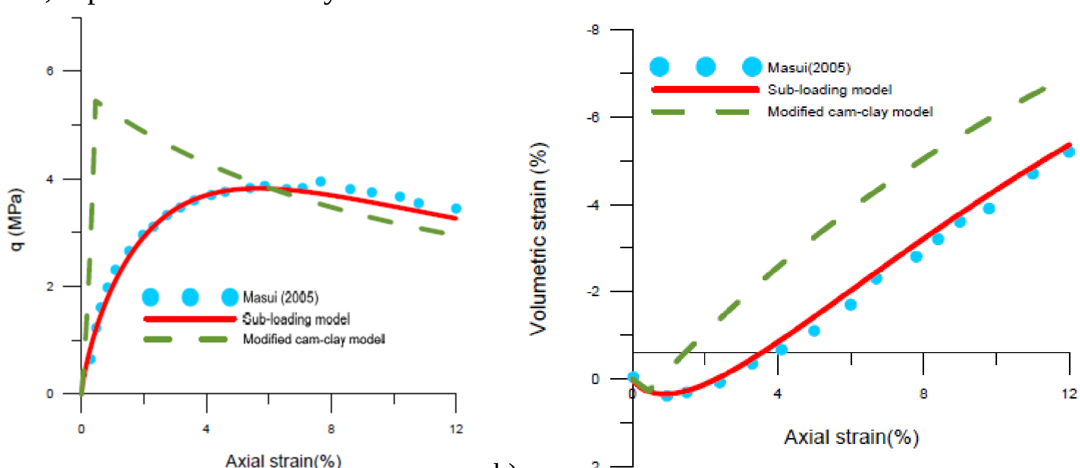

a) b)

Figure 1. Modeling the drained triaxial test on pure Toyoura sand (Masui et al., 2005) using the MCC and sub-loading models: a) stress strain behavior, and b) volumetric behavior.

The main parameters adopted for the numerical analysis are presented in Table 2. The porosity (*n*) values reported by Masui et al. (2005) were between 37.7 and 42.4%.

Table 2. Soil parameters adopted in the modeling of Toyoura sand specimens

Properties	Sub-loading model	MCC model
λ	0.16	0.16
κ	0.004	0.004
M	1.07	1.07
p_c (MPa)	12	12
n	0.38	0.38
G (MPa)	0.75K	0.75K
u	15	-

To validate the implementation of the sub-loading model for sediments containing gas hydrates, two more tests carried out by Masui et al. (2005) were selected. One of this synthetic samples was prepared using the ice-seed method (i.e. a pore filling dominating sample was obtained), and the other one was formed using the partial water saturation method (i.e. a cementing dominating sample was obtained). Figure 2 shows with symbols that stress-strain relationship and volumetric behavior of hydrate-bearing Toyoura sands reported in Masui et al. (2005). Both samples have the same hydrate saturation. The model outputs obtained with the sub-loading model are also presented in this figure, using continuous lines. It can be seen that the model is able to capture very well the different features of HBS behavior observed in these experiments between the pore-filling and cementing specimens, particularly in terms of peak deviatoric stresses.

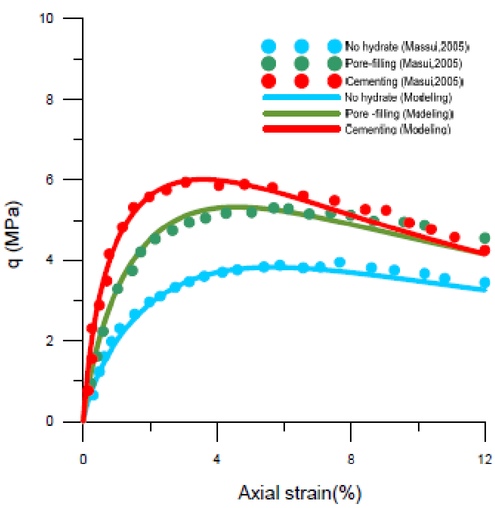

a)

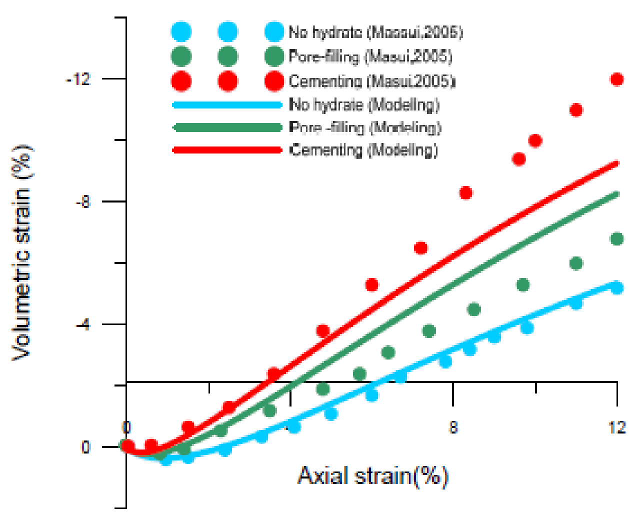

b)

Figure 2. Modeling the drained triaxial tests on pure Toyoura sand and hydrate samples (Masui et al., 2005) using the sub-loading model: a) stress strain behavior, b) volumetric behavior.

The model also captures well the tendencies observed in terms of soil dilatancy, with slight model over-predictions. In order to reproduce the different behaviors observed between pore-filling and cementing specimens, it is necessary to adopt different hardening strength parameters p_d. Table 3 presents the parameters adopted in the modeling.

Table 3 Soil parameters adopted in the modeling of HBS specimens

Properties	Pore-filling specimen	Cementing specimen
λ	0.16	0.16
κ	0.004	0.004
M	1.07	1.07
p_c (MPa)	12	12
n	0.38	0.38
G (MPa)	0.75K	0.75K
u	15	15
a	18	62
b	1.6	1.6

Reference:

Hashiguchi K. (1989). Subloading surface model in unconventional plasticity. Int. J. Solids Structure. 25(8): 917–945.

Hyodo M., Nakata Y., Yoshimoto N., and Ebinuma T. (2005). Basic research on the mechanical behavior of methane hydrate-sediments mixture. Soils and foundations, 45(1), 75-85.

Hyodo M., Nakata Y., Yoshimoto N., and Yoneda J. (2008) Shear Strength of methane hydrate bearing sand and its deformation during dissociation of methane hydrate. 549-556.

Masui A., Haneda H., Ogata Y. and Aoki K. (2005). Effects of methane hydrate formation on shear strength of synthetic methane hydrate sediments. Proceedings of the Fifteenth International Offshore and Polar Engineering Conference, International Society of Offshore and Polar Engineers, Seoul, Korea.

Miyazaki K., Tenma N., Aoki K. and Yamaguchi T. (2012). A nonlinear elastic model for triaxial compressive properties of artificial methane-hydrate-bearing sediment samples. Energies, 5(10): 4057-4075.

Pinkert, S. and J. Grozic, Prediction of the mechanical response of hydrate-bearing sands. Journal of Geophysical Research: Solid Earth, 2014. 119(6): 4695-4707.

Roscoe K. H. and J. B. Burland (1968). On the generalized stress-strain behavior of ‘wet’ clay. Cambridge Univ. Press, Cambridge, U. K.

Roscoe K.H., Schofield A.N, and Wroth C.P. (1958). On the yielding of soils. Géotechnique, 8(1), 22–53

Uchida S., Soga K. and Yamamoto K. (2012). Critical state soil constitutive model for methane hydrate soil. Journal of Geophysical Research: Solid Earth (1978–2012), 117(B3).

Yoneda J., Hyodo M., Nakata Y. and Yoshimoto N. (2010). Triaxial Shear Characteristics of Methane Hydrate-bearing Sediment in the Deep Seabed, Journal of Geotechnical and Geoenvironmental Engineering, Vol.66, No.4, pp.742-756.

Waite W., Santamarina J.C., Cortes D., Dugan B., Espinoza D., Germaine J., Jang J., Jung J., Kneafsey T., Shin H., Soga K., Winters W., Yun T. Physical properties of hydrate-bearing sediments. Review. Geophysics, 47(4), RG4003, doi:10.1029/2008RG000279.

Benchmark Test 2

We have started with the validation of our code using the benchmarks prepared in the context of "The National Methane Hydrates R&D Program: Methane Hydrate Reservoir Simulator Code Comparison Study" (http://www.netl.doe.gov/technologies/oil-gas/FutureSupply/MethaneHydrates/MH_CodeCompare/MH_CodeCompare.html

Benchmark Test # 2 is related to the analysis of "Closed-Domain Hydrate Dissociation (Base Case w/ Hydrate)". We are copying below the description of Benchmark Test # 2

One half of a 20-m, one-dimensional horizontal domain, discretized using uniformly spaced 1-m grid cells (optionally 0.1-m grid cells) is initialized with aqueous-hydrate conditions; whereas, the other half of the domain is initialized with gas-aqueous conditions. As with the Base Case problem, a closed horizontal domain is used to eliminate gravitational body forces and boundary condition effects. The initial conditions are specified to yield complete dissociation of the hydrate, via the thermal capacitance of the domain-half initialized with gas-aqueous conditions. To initialize the aqueous-hydrate half of the domain, temperature, pressure, and hydrate saturation are specified. For reference purpose hydrate equilibrium pressure, hydration number, and cage occupancies will also be specified for this half of the domain. To initialize the gas aqueous half of the domain temperature, aqueous pressure and gas pressure are specified. All active phases (i.e., aqueous, gas, and hydrate) are assumed to comprise water and CH4, and capillarity is assumed between the active phases. Hydrate dissociation is assumed to occur using equilibrium kinetics (i.e., infinitely fast dissociation rates). From the specified initial conditions, the simulations proceeds to equilibrium conditions in temperature and pressure, dissociating the hydrate during the transition process and leaving gas-aqueous conditions. Variable time stepping should be used to capture the flow and transport processes at early and late times during simulation. A schematic of the initial conditions for the problem are shown in Figure 2.1 and problem parameters and specifications are provided in Table 2.1. In Figure 2.1 the specified initial condition parameters are listed above the domain region and the computed initial condition parameters are listed for reference inside the domain region. The computed initial condition parameters are computable from the specified initial condition parameters.

The list of processes simulated in this problem include:

5. multifluid flow for an aqueous-gas-hydrate system in geological media, subject to relative permeability and capillarity effects and phase transitions,

6. dissociation of CH4 hydrate in response to thermal stimulation and depressurization,

7. heat transport across multifluid geological media with phase advection and component diffusion,

8. change in CH4 solubility in water with pressure and temperature,

9. change in thermodynamic and transport properties with pressure and temperature.

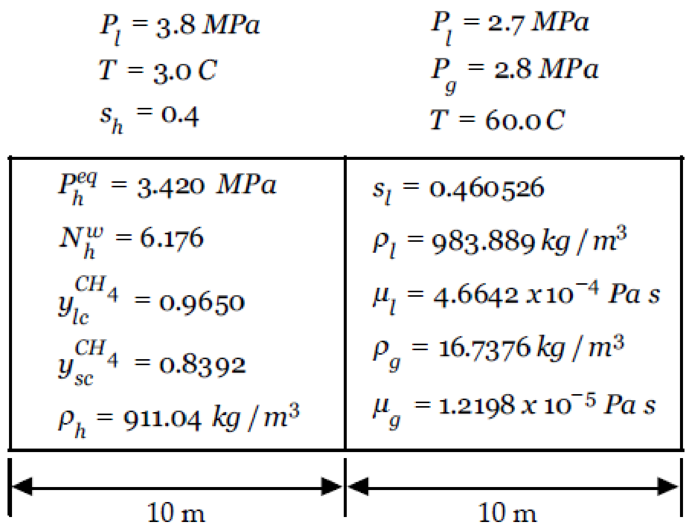

Figure 2.1. Problem Schematic

Figure 3. Schematic representation as reported in Benchmark #2

Simulation Results

Figure 4, 5 and 6 present the comparisons between the simulators that took part of the benchmark (i.e. HydrateResSim,MH-21,stars-Mehran,STARS,STOMP-HYD,TOUGH-FX,Univ-Houston) and 'THCM-hydrate' (the simulator that is being developed in the context of this project) in terms of temperature, gas pressure and hydrate saturation, respectively. The results with symbols correspond to THCM-hydrate. The performance of THCM-hydrate' can be considered very satisfactory, there are some slight differences, but the main patterns of the system behavior are well captured by the model. More details about this case can be found in the webpage with the benchmarks results (http://www.netl.doe.gov/research/oil-and-gas/methane-hydrates/mh-codecompare).

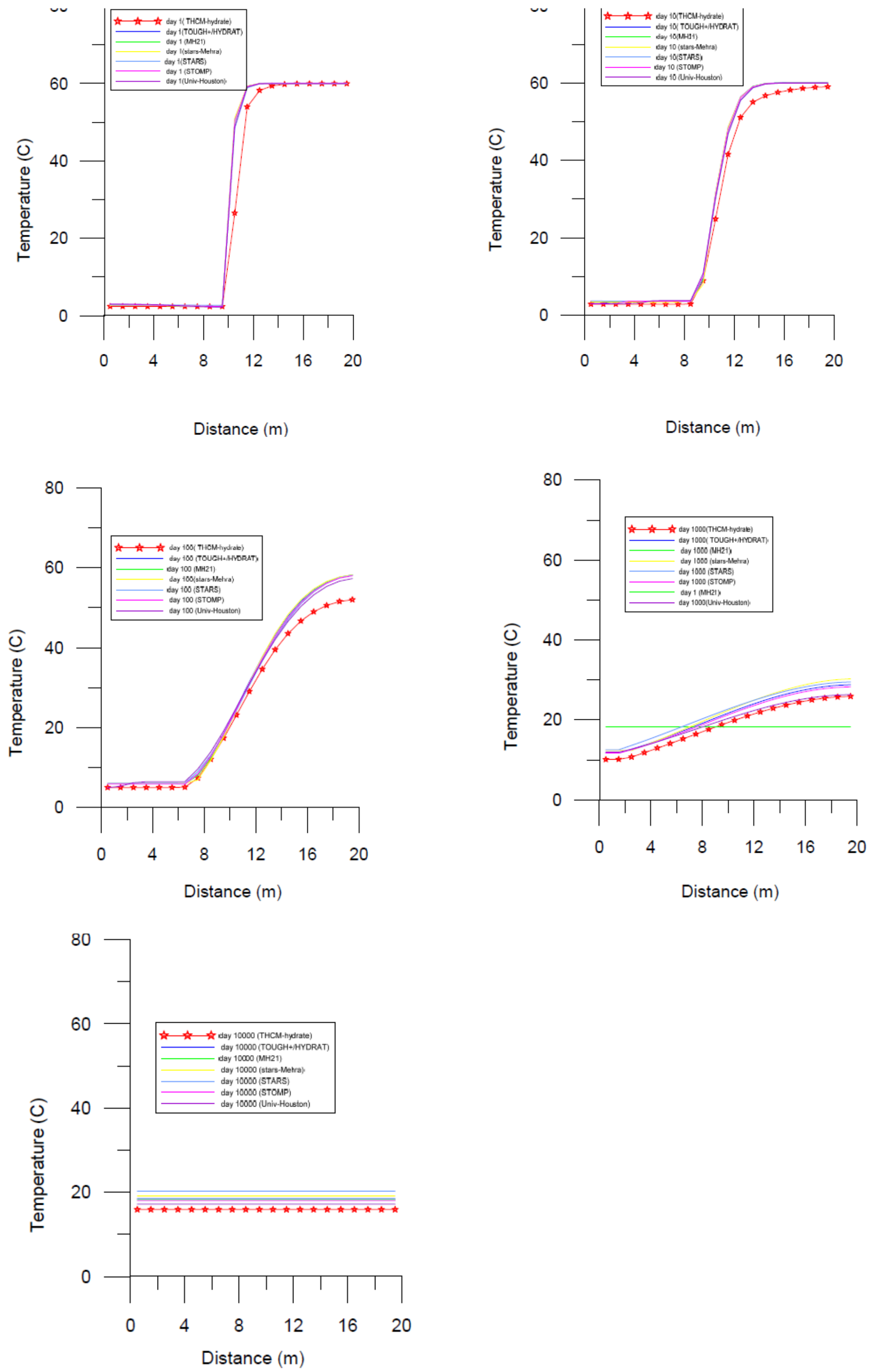

Figure 4. Simulators results comparisons in terms of temperature

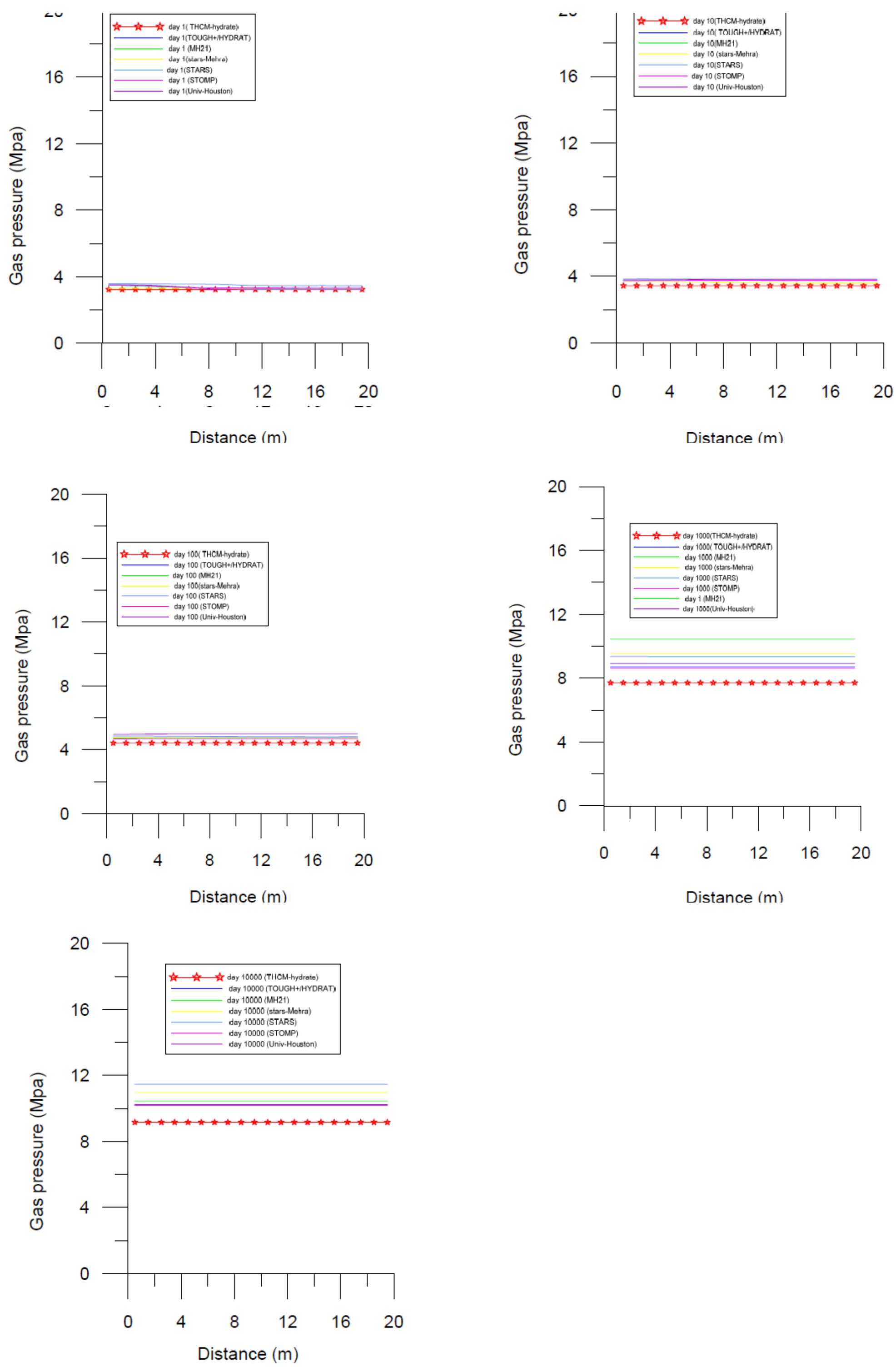

Figure 5. Simulators results comparisons in terms of gas pressure

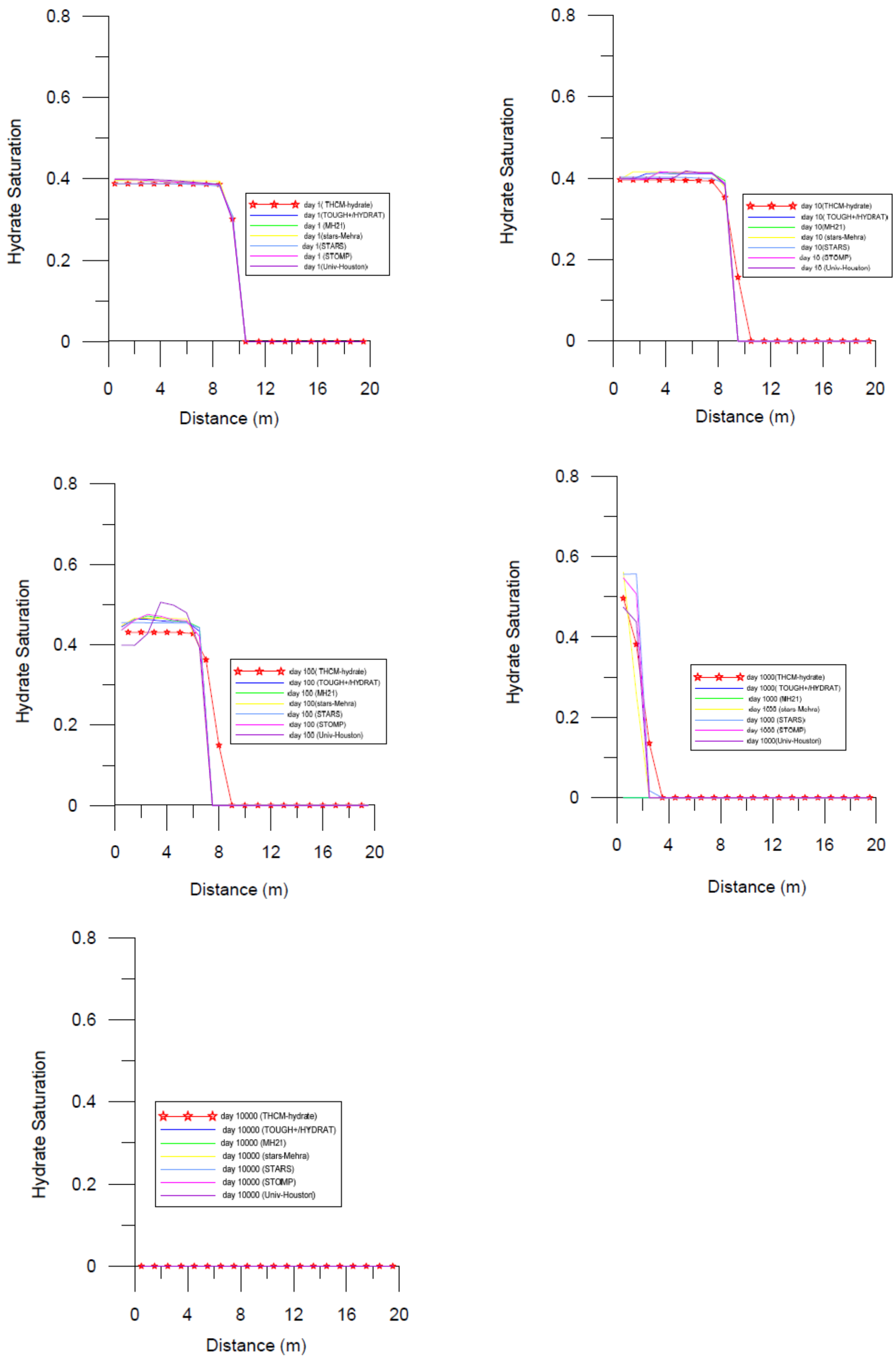

Figure 6. Simulators results comparisons in terms of SH

PRODUCTS

Publications – Presentations:

- A conference paper has been accepted at the XVI ECSMGE 2015. Edinburgh, UK, September 13-17 2015 Title: "Numerical Modeling of Gas Hydrate Bearing Sediments". Authors: M. Sanchez, J. C. Santamarina. A. Shastri & Xuerui Gai.

Website: Publications (for academic purposes only) and key presentations are included in http://pmrl.ce.gatech.edu/; http://ceprofs.civil.tamu.edu/msanchez/

Technologies or techniques: None at this point.

Inventions, patent applications, and/or licenses: None at this point.

Other products: None at this point.

PARTICIPANTS

Research Team: The current team is shown next.

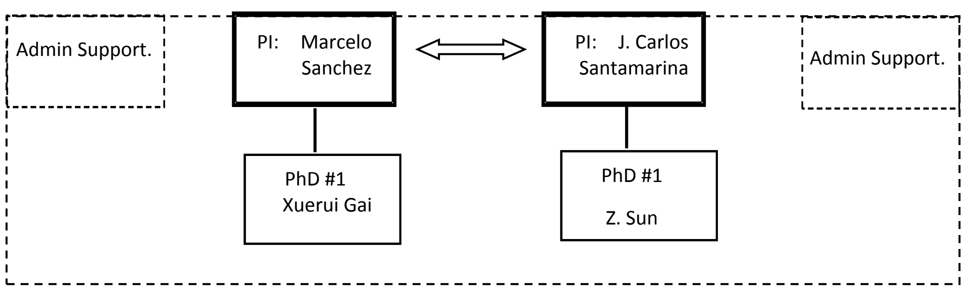

IMPACT

- While it is still too early to assess impact, we can already highlight the computational platform extensively validated in a wide range of coupled thermo-hydro-chemo-mechanical coupled problems (CB_Hydrate).

CHANGES/PROBLEMS:

None so far.

SPECIAL REPORTING REQUIREMENTS:

Nothing to report

BUDGETARY INFORMATION:

TAMU

				Budget Period 1								Budget Period 2
	Q1		Q2		Q3		Q4		Q1		Q2	
	Enter date range		Enter date range		Enter date range		Enter date range		Enter date range		Enter date range	
Baseline Reporting Quarter	10/1/13-12/31/13		01/01/14-03/31/14		04/01/14-06/30/14		07/01/14-9/30/14		10/1/14-12/31/2014		01/01/15-03/31/15	
	Q1	Cumulative Total	Q2	Cumulative Total	Q3	Cumulative Total	Q4	Cumulative Total	Q1	Cumulative Total	Q2	Cumulative Total
Baseline Cost Plan	$ 30,300.00	$30,300.00	$30,300.00	$60,600.00	$ 30,300.00	$ 90,900.00	$ 88,667.00	$179,567.00	$ 37,800.00	$217,367.00	$ 37,800.00	$ 255,167.00
Federal Share	$ 30,300.00	$30,300.00	$30,300.00	$60,600.00	$ 30,300.00	$ 90,900.00	$ 88,667.00	$179,567.00	$ 37,800.00	$217,367.00	$ 37,800.00	$ 255,167.00
Non-Federal Share	$ 11,223.00	$11,223.00	$11,223.00	$22,446.00	$ 11,223.00	$ 33,669.00	$ 11,223.00	$ 44,892.00	$ 11,223.00	$ 56,115.00	$ 11,223.00	$ 67,338.00
Total Planned	$ 41,523.00	$41,523.00	$41,523.00	$83,046.00	$ 41,523.00	$124,569.00	$ 99,890.00	$224,459.00	$ 49,023.00	$273,482.00	$ 49,023.00	$ 322,505.00
Actual Incurred Costs	$ 5,301.83	$ 5,301.83	$13,764.34	$19,066.17	$ 33,827.48	$ 52,893.65	$ 51,567.77	$104,461.42	$ 80,352.17	$184,813.59	$ 24,626.18	$ 209,439.77
Federal Share	$ 3,335.02	$ 3,335.02	$ 9,848.68	$13,183.70	$ 10,170.37	$ 23,354.07	$ 58,205.62	$ 81,559.69	$ 92,208.79	$173,768.48	$ 31,359.66	$ 205,128.14
Non-Federal Share	$ 5,182.96	$ 5,182.96	$20,751.77	$25,934.73	$ 20,743.19	$ 46,677.92	$ 29,262.19	$ 75,940.11	$ -	$ 75,940.11	$ -	$ 75,940.11
Total Incurred costs	$ 8,517.98	$ 8,517.98	$30,600.45	$39,118.43	$ 30,913.56	$ 70,031.99	$ 87,467.81	$157,499.80	$ 92,208.79	$249,708.59	$ 31,359.66	$ 281,068.25
Varience	$ 33,005.02	$33,005.02	$10,922.55	$43,927.57	$ 10,609.44	$ 54,537.01	$ 12,422.19	$ 66,959.20	$(43,185.79)	$ 23,773.41	$ 49,023.00	$ 41,436.75
Federal Share	$ 1,966.81	$ 1,966.81	$ 3,915.66	$ 5,882.47	$ 23,657.11	$ 29,539.58	$ (6,637.85)	$ 22,901.73	$ 11,045.11	$ 33,946.84	$ (6,733.48)	$ 4,311.63
Non-Federal Share	$ 6,040.04	$ 6,040.04	$ (9,528.77)	$ (3,488.73)	$ (9,520.19)	$ (13,008.92)	$(40,485.19)	$ (53,494.11)	$ 11,223.00	$(42,271.11)	$ 11,223.00	$ (31,048.11)
Total Varience	$ 8,006.85	$ 8,006.85	$ (5,613.11)	$ 2,393.74	$ 14,136.92	$ 16,530.66	$(47,123.04)	$ (30,592.38)	$ 22,268.11	$ (8,324.27)	$ 13,943.84	$ 5,619.57

GT

Baseline Reporting Quarter DE-FE0013889	Budget Period 1								Budget Period 2							
	Q1		Q2		Q3		Q4		Q1		Q2		Q3		Q4	
	10/1/13 - 12/31/13		1/1/14 - 3/31/14		4/1/14 - 6/30/14		7/1/14 - 9/30/14		10/1/14 - 12/31/14		1/1/15 - 3/31/15		4/1/15 - 6/30/15		7/1/15 - 9/30/15	
	Q1	Cumulative Total	Q2	Cumulative Total	Q3	Cumulative Total	Q4	Cumulative Total	Q1	Cumulative Total	Q2	Cumulative Total	Q3	Cumulative Total	Q4	Cumulative Total
Baseline Cost Plan																
Federal Share	21,556	21,556	21,556	43,112	21,556	64,667	21,556	86,223	18,000	104,223	18,000	122,223	18,000	140,223	34,658	174,881
Non-Federal Share	7,315	7,315	7,315	14,630	7,316	21,946	7,316	29,262	7,535	36,797	7,535	44,332	7,535	51,866	14,100	65,966
Total Planned	28,871	28,871	28,871	57,742	28,872	86,613	28,872	115,485	25,535	141,020	25,535	166,555	25,535	192,089	48,758	240,847
Actual Incurred Cost																
Federal Share	0	0	11,228	11,228	11,458	22,685	48,488	71,174	21,192	92,366	2,131	94,497				
Non-Federal Share	0	0	0	0	21,946	21,946	-20	21,926	16,170	38,096	0	38,096				
Total Incurred Costs	0	0	11,228	11,228	33,404	44,631	48,468	93,099	37,362	130,461	2,131	132,592				
Variance																
Federal Share	-21,556	-21,556	-10,328	-31,884	-10,098	-41,982	26,933	-15,049	3,192	-11,857	-15,869	-27,726				
Non-Federal Share	-7,315	-7,315	-7,315	-14,630	14,630	0	-7,336	-7,336	8,635	1,299	-7,535	-6,236				
Total Variance	-28,871	-28,871	-17,643	-46,514	4,532	-41,982	19,596	-22,386	11,827	-10,559	-23,404	-33,962				

National Energy Technology Laboratory

626 Cochrans Mill Road
P.O. Box 10940
Pittsburgh, PA 15236-0940

3610 Collins Ferry Road
P.O. Box 880
Morgantown, WV 26507-0880

13131 Dairy Ashford Road, Suite 225
Sugar Land, TX 77478

1450 Queen Avenue SW
Albany, OR 97321-2198

Arctic Energy Office
420 L Street, Suite 305
Anchorage, AK 99501

Visit the NETL website at:

www.netl.doe.gov

Customer Service Line:

1-800-553-7681